

# Three-Component LDA Measurements in an Axial-Flow Compressor

Christopher J. Chesnakas\* and Clinton L. Dancy†

*Virginia Polytechnic Institute and State University, Blacksburg, Virginia 24061*

A three-color, three-component laser Doppler anemometer (LDA) was used to simultaneously measure the three components of velocity in a low speed (2900 rpm), axial-flow-compressor, rotor-blade passage. It is demonstrated that accurate measurements in the mean motion are possible over much of the blade passage and that the secondary motions can be captured. Confirmation of the observed mean-flow results is obtained through a comparison of the three-dimensional flow with limited stationary pressure probe measurements and simple irrotational flow assumptions. The presentation of the measurements is followed by a discussion of the difficulties encountered in making simultaneous three-component velocity measurements in blade passages with LDA, and suggestions are made for improving the present system for this task.

## Nomenclature

$h_{ms}$	= distance of the measurement point above the blade suction surface
$h_{ps}$	= distance from the blade suction surface to an adjacent blade pressure surface
$P$	= pressure
$p$	= probability
$Q$	= ratio of the required number of fringe crossings to the total present
$r$	= radial coordinate
$t$	= tangential coordinate
$U$	= blade velocity magnitude
$V$	= particle velocity
$V_F$	= fringe velocity
$x$	= axial coordinate
$\alpha_p$	= angle of the blade pressure surface to the horizontal
$\alpha_s$	= angle of the blade suction surface to the horizontal
$\theta$	= angular coordinate
$\rho$	= density
$\psi$	= angle between the particle velocity and the fringe normal

## Subscripts

$b$	= blue, 488-nm channel
$g$	= green, 514.5-nm channel
$o$	= stagnation conditions
$r$	= radial component
tip	= evaluate at the blade tip
$v$	= violet, 476.5-nm channel
$x$	= axial component
$\theta$	= azimuthal component

## Introduction

**D**UE to the increasing demand for improved performance and efficiency in air-breathing jet engines, there is a growing need for methods to study and analyze the detailed

flow behavior in rotating machines. Three-dimensional computational analysis of the flow in axial-flow machines is now possible, and the development and application of these computational methods is already vital to the continued development of advanced propulsion concepts. On the experimental side of this development process, there is an obvious need for accurate, detailed measurements of the three-dimensional flowfield in these rotating environments.

The laser Doppler anemometer (LDA) in rotating machines is of course now commonplace, although in most cases only two components of the mean velocity (axial and tangential) in the blade row are obtained. The literature for two-component LDA measurement in axial flow machines is readily available<sup>1</sup> and not reviewed here. A number of such studies have appeared in previous issues of the present journal. There are exceptions however where all three mean velocity components have been measured. Stauter and Fleeter<sup>2</sup> measured the three components of velocity in an annular cascade using a one-component LDA by making measurements at several successive angular orientations. Carey et al.<sup>3</sup> reported the measurement of the three components of mean velocity in a mixed-flow compressor using a two-component LDA in two different orientations. These examples represent situations where all three components of velocity were obtained successively rather than simultaneously, the latter procedure having definite advantages. Although three-component LDA systems are now available and their application to a wide variety of research studies is growing,<sup>4,5</sup> the application of simultaneous three-component LDA to turbomachinery has been slow.

In the present paper, the results of the application of a three-component LDA to the simultaneous measurement of the three components of velocity in an axial-flow research compressor are presented. The facilities and equipment are discussed first and followed by the results of the uncertainty analysis, the measurement results, and conclusions.

## Equipment and Facilities

The research compressor was a modified General Electric model 5GDY34A1 axial-flow fan/dynamometer set, configured as a single-stage rotor and stator. A speed variator allowed speeds up to 3000 rpm. The hub radius was 15.65 cm, and the inner casing radius was 22.73 cm. The single-fan stage consisted of a 24-blade rotor with RAF-6 propeller blade profiles with 4 deg of twist and a midspan stagger angle of 45.5 deg. The 37-blade stator was located 26 mm behind the rotor. The rotor blades have a chord length of 43.36 mm and a maximum thickness of 5.56 mm. Rotor solidity was 0.84. At

Presented as Paper 88-2811 at the AIAA/ASME/SAE/ASEE 24th Joint Propulsion Conference, Boston, MA, July 11-13, 1988; received July 25, 1988; revision received May 4, 1989. Copyright © 1988 by the American Institute of Aeronautics and Astronautics, Inc. All rights reserved.

\*Graduate Research Assistant, Department of Mechanical Engineering.

†Assistant Professor, Department of Mechanical Engineering. Member AIAA.

the operation speed of 2900 rpm, the tip speed was 69.0 m/s. There was a 0.6 mm tip gap between the rotor and casing. The stator section had a midspan solidity of 1.36, a midspan stagger angle of 15 deg with 8 deg of twist, and a turning angle of 27 deg. The compressor flow was throttled downstream and then discharged into the laboratory.

To allow optical access to the rotor blade passage, the compressor was modified with the addition of a 6.4-mm-thick uncoated plexiglass window. The flat window was flush with the inner casing wall at midheight and deviated from the contour of the cylindrical casing by 0.80 mm at the top and bottom. The dimensions allowed optical access from 17 mm in front of the leading edge of the rotor ( $-0.55$  axial chord) to 12 mm behind the rotor trailing edge (1.40 axial chord) and from 45% span out to the blade tip.

At the operating speed of 2900 rpm, the compressor characteristic is flat from the incipient stall  $V_x/U_{tip}$  of 0.36 to the maximum  $V_x/U_{tip}$  of 0.47. Over this range, the total pressure rise is a nearly flat  $\Delta P_O/0.5\rho U_{tip}^2 = 0.482$ . At wide open throttle, the angle between the chord line and the relative velocity vector (the angle of attack) was 13 deg at 12% span and 22 deg at 84% span; at incipient stall, the angle of attack increased to 19 deg at 12% span and 26 deg at 84% span.

The LDA measurements were made at a  $V_x/U_{tip}$  of 0.44. Typically, the temperature was 28°C, and the barometric pressure was 709 mm Hg. At this operating condition, the angle of attack was 14 deg at 12% span and 23 deg at 84% span.

Stationary three-hole pressure probe measurements were made in front of the leading edge of the rotor. These measurements showed that the inlet axial velocity was uniform from hub to tip. However, similar measurements behind the rotor indicated a strong radial dependency with the tip region carrying more mass than the hub region.

More detail on this compressor configuration and the compressor performance can be obtained from internal reports and departmental theses. References for such works can be found in Ng et al.<sup>6</sup> where in addition it is shown by "on rotor" pressure measurements that a stator-rotor interaction is present due to the close proximity of the stator and rotor blading. The details of this interaction are not however the subject of the present work.

The LDA used for these tests is a three-color, three-component TSI system 9100-12. The 488-nm, 514.5-nm and 476.5-nm lines are used in what is essentially three dual beam systems. It can be seen from Fig. 1 that the blue and green beams are transmitted along a common optical axis and measure velocity components which are mutually perpendicular. The violet beams are transmitted along a separate optical axis and

measure a component which is perpendicular to that measured by the blue beams, but not the green. The angle between the blue/green optical axis and a normal to the compressor axis was 13 deg 20 min, and the violet optical axis was at 25 deg 58 min to the compressor axis for a total separation of the nonorthogonal violet and green components of 39 deg 18 min. Off-axis backscatter collection was employed. Total laser output power was set to 1.5 watts for all reported measurements.

The laser and all optics were mounted on a single optical table which was attached to a mechanical traversing mechanism. With this device, the optical table could be moved both in a direction parallel to the compressor axis, the  $x$  direction, and in a direction perpendicular to the compressor axis, the  $r$  direction. Manually powered machine screws attached to a dial index allowed positioning to  $\pm 0.05$  mm. The freedom of the table to move in the  $x$  or  $r$  directions, combined with the rotation of the blade passage, allowed for three degrees of freedom of movement within the blade passage. In addition the optical table could be rotated about the  $r$  axis. In order to increase optical access to the blade passage, the table was positioned at a fixed rotation of 45 deg 25 min, approximately the stagger angle of the blades.

Before signal analysis the Bragg shifted Doppler signals were downmixed to provide an effective frequency shift of from 0–10 MHz, and the signals were bandpass filtered. Counter processors were used with 2% comparison, and eight fringe crossings were used for each individual burst. Measurements were only accepted when all three channels recorded bursts within a 50  $\mu$ s coincidence window.

The position of the compressor shaft was encoded, and one shaft revolution was divided into 480 measurement zones so that each blade passage contained 20 (480/24) measurement zones or what will be termed gated windows. Data were recorded only when a gated window was enabled. At midspan, each of these gated windows is 2.5 mm in length, which corresponds to a 43  $\mu$ s duration. This relatively large gated window size was chosen to increase data rate at the expense of spatial resolution. Likewise, data were averaged over all blade passages in order to increase the data rate.

Data were acquired in groups of 256 bursts by a PDP 11/24 digital computer with direct memory access. Because the LDA system was operated in coincidence mode, each recorded burst consisted of three measurements, one for each of the three measured components of velocity. At each measurement location, 4 groups of data, or 1024 data points, were taken.

It is emphasized that the gated encoder window results in a spatial average of the LDA data over this window. The coincidence time window is independent of the encoder gated win-

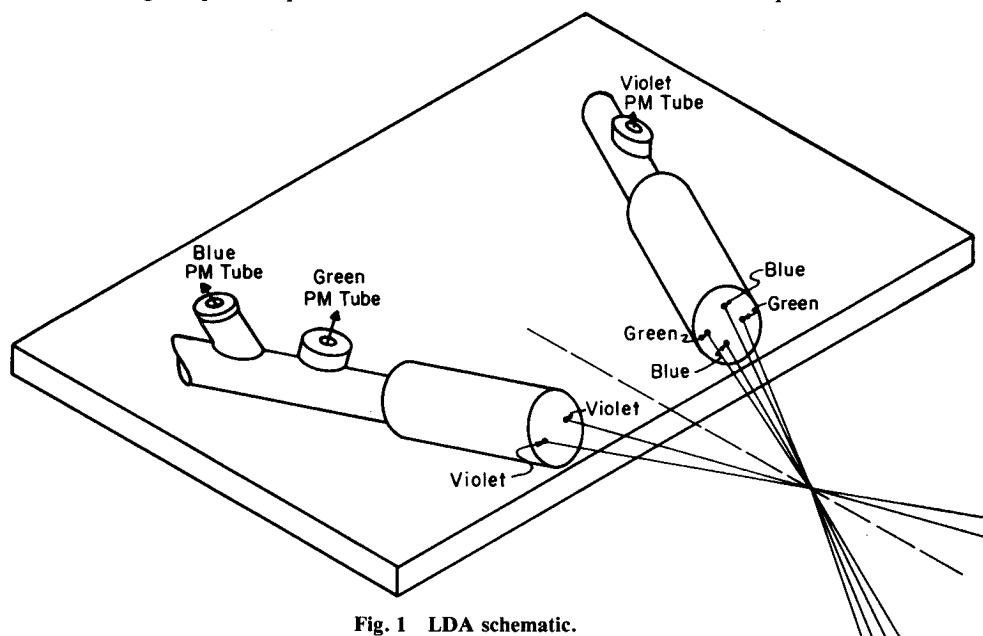


Fig. 1 LDA schematic.

dow but is of comparable size at the operational speed of rotation. Since only mean velocity results, and not higher level turbulence quantities, are being reported and with the coincidence time window comparable to the encoder gated window, there is no additional uncertainty in the mean velocities due to the coincidence window size beyond that due to spatial averaging. The error associated with velocity gradients over the LDA measurement volume has been investigated by Kreid.<sup>7</sup> In the present flow, a comparable error due to gradients over the gated window is difficult to estimate without more detailed measurements or computational models of this machine.

As mentioned above, the flow from the compressor dumped directly into the room. Sugar seed was used and generated by supplying a six jet aerosol seeder with a solution of sugar and water. The spherical shape of the resulting solid sugar particles and the seed size distribution were determined by scanning electron microscope photographs of the seed collected on glass observation slides. Aerodynamic particle sizing was also performed later in the study. Sizes on the order of 2  $\mu\text{m}$  and less were prevalent.

Seed was introduced locally to the flow about 15 cm upstream of the compressor bellmouth. Seeding the flow in this way, the maximum data rate was about 500 per s when collecting data in a single window and averaging over all blades. When no windowing was used, the data rate was about 20 times the windowed rate, or 10,000 per second. With this data rate, the probability of two particles being in the probe volume at any one time was estimated to be 0.02%.

The upstream location for seed injection was determined by observation of the measured velocities and variances near the leading edge of the rotor. The injection position was located upstream of the bellmouth inlet at such a position to minimize flow disturbance at the measurement location and still maintain some control over seed trajectory. The evaporation of the water to assure solid sugar at the measurement location was tested by running with pure water.

As the rate of evaporation depends upon the ambient air humidity, which may vary from day to day, if very precise measurements are sought, regular tests for complete evaporation are recommended. Laboratory conditions on scheduled test days were monitored so that consistent seeding performance could be anticipated; although regular daily tests for complete evaporation of pure water were not performed. For greatest precision, injection of a polystyrene latex (PSL) monodisperse seed is preferable, although this was avoided here for health reasons.

### Measurement Uncertainty

The analysis of the velocity uncertainty requires knowledge of the uncertainty in the angles among the optical axes, individual component beam angles, clock count uncertainty, fringe divergence, and downmixer accuracy, in addition to possible other sources as discussed in the literature.<sup>8</sup> The analysis is straightforward but tedious and so is not detailed here.

Because of the limitations on optical access to the blade passage, none of the velocity components of interest were measured directly. Instead, particle transit times corresponding to three nonorthogonal velocity components,  $V_b$ ,  $V_g$ , and  $V_v$ , were measured. The transformation between the measured particle transit times and the orthogonal  $x$ - $t$ - $r$  velocity components is a function of several angles including the angles between the six beams and the angles between the LDA and the compressor. This transformation and the uncertainty analysis are covered in detail in Chesnakas.<sup>9</sup> In the present case, the uncertainty in any *measured* component is associated almost entirely with the uncertainty in the fringe spacing. The half angle of any component beam system was measured to  $\pm 2$  min, and the downmixer, counter clock, and bit truncation errors were extremely small for representative burst frequencies. The resulting uncertainty in any *measured* velocity is  $\pm 1.2\%$ .

To determine the uncertainty in the computed orthogonal components, the uncertainties in the measured velocities and in the measured angles were propagated through the transformation equations. The final uncertainties in the orthogonal  $x$ ,  $t$ , and  $r$  components were found to be relatively insensitive to the angle between a given optical axis and the axis of the machine. Of all variables affecting the uncertainty, the coupling angle between the green and violet channels (approximately 40 deg in the present case) is the most important parameter. The axial and tangential components are relatively insensitive to coupling angle, but the radial component is dominated by the coupling angle sensitivity. This possibility of large uncertainty in the radial component for small coupling angles was predicted by previous researchers.<sup>10</sup> The coupling angle used in this work was chosen to reduce this uncertainty without seriously compromising optical access.

The error analysis shows that the uncertainty in velocity varies with the swirl of the flow and thus with the position of the measurement. The uncertainties in the axial and tangential components are roughly equal at 0.3 m/s at the entrance to the blade passage where the flow has very little swirl and 0.4 m/s at the exit of the blade passage. These are both approximately equal to 1% of the *total* velocity. The uncertainty in the radial component is more sensitive to swirl angle and is 0.6 m/s at the entrance to the blade passage and 0.2 m/s at the exit. As a relative uncertainty, this can be quite large as the radial velocity rarely exceeds 4 m/s.

Another source of error is the statistical biasing effect in LDA measurements of turbulent flows known as fringe, or angular, bias. Ideally, the mean flow should be perpendicular to the fringes to minimize this biasing effect. For a three component measurement, this ideal is impossible to achieve simultaneously on all three channels. Therefore, angular bias effects must be considered.

Petrie et al.<sup>11</sup> have estimated the probability of making a measurement on a particle traveling at an angle  $\psi$  to the fringe normal to be

$$p = 1 - \frac{Q^2}{[\cos \psi - (V_F/V)]^2} \quad (1)$$

For a three-component system in coincidence mode, the probability of making a velocity measurement can be estimated by the product of the probabilities for each of the three channels.

For the current system, the total number of fringes was estimated to be approximately 13 for all colors. In order to examine the effect of angular bias on the flow through the compressor, an "average" flow through the blades was examined. The flow was assumed to have no swirl at the entrance to the blade passage. It was taken as a function of axial position only and was assumed to emerge from the blade passage with a swirl of  $-41$  deg. The axial velocity was constant at 30.9 m/s throughout. Figure 2 shows the probability of making a velocity measurement in this average assumed flow as a function of swirl angle for varying frequency shifts for each channel. It is observed that as the flow approaches large negative swirl angles (which occurs in the test compressor), the probability of making a measurement on the green and violet channels drops to zero unless frequency shift is employed. The error induced from angular bias is not accurately or easily quantified; therefore, the analysis above was used 1) to recognize under what conditions bias is a problem so that proper shifting could be used and 2) to determine if data already taken was badly fringe biased. Just as for velocity bias, fringe bias becomes more serious as turbulence increases.

Since an LDA does not actually measure the velocity of the flow, but rather measures the velocity of particles suspended within the flow, particle lag must be estimated. In order to estimate the particle lag in this flow, the motion of a particle traveling through a blade passage was numerically simulated. Since, at the time this simulation was performed, the detail of the flow through a blade passage was unknown, an average

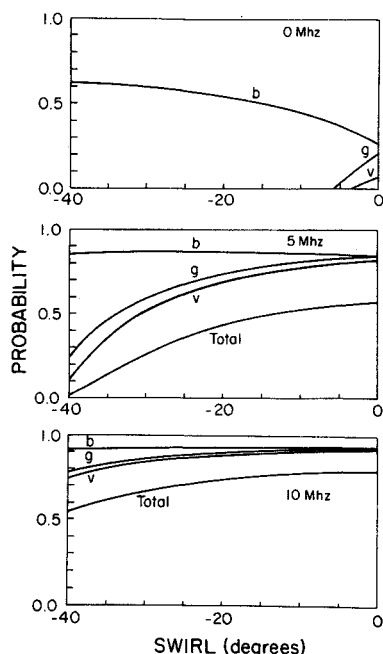


Fig. 2 Measurement probability due to angular bias.

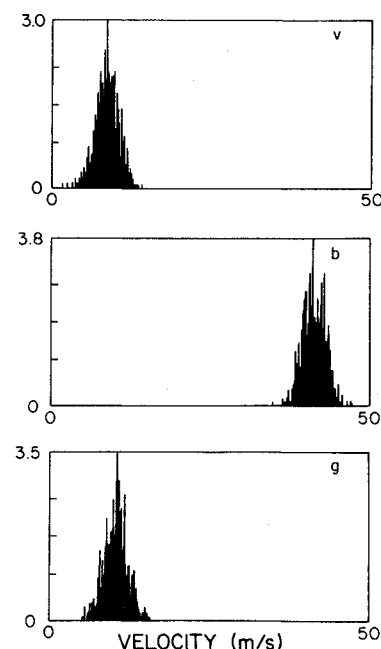


Fig. 3 Velocity histograms, 62.5% span, 71.3% axial chord.

flow through the blade passage, as derived from three-hole probe measurements taken before and after the rotor, was assumed.

In the numerical simulation, the particle was assumed to have zero lag at the entrance to the blade passage, and the lag of the particle was tracked throughout. Particles from 1–5  $\mu$  in diameter were simulated. The analysis showed that in this low-speed compressor, particle lag only becomes significant—velocity deviation of greater than 1% and angular deviation of greater than 1 deg—as particle size exceeds 2  $\mu$ . Furthermore the induced radial velocity (assumed zero at the entrance) due to particle inertia is approximately 0.1 m/s at the compressor exit. As the measured radial velocities were on the order of 3–4 m/s, typically, it was concluded that particle lag effects on the mean velocities are not significant for this study.

No velocity bias correction was employed in the reported data. Over most of the blade passage, it is estimated that the uncertainty due to velocity bias is less than 1%.

In addition to the uncertainties discussed above, there is also the statistical error associated with the finite sample size used for estimating the mean velocities. This error was estimated by computing the standard error of the mean using 1024 points per location. Using a 95% confidence level for this estimation and combining this error with the previous uncertainties in a sum of squares manner results in representative uncertainties in the orthogonal mean velocities of 2% and 4% in the axial and tangential components and 20% in the radial at the leading edge; 2% and 3% in axial and tangential and 20% in the radial at the blade row exit.

## Results

Data were collected at seven axial locations: –43.4, –0.02, 22.1, 41.8, 71.3, 100.0, and 120.5% of the axial chord length. At each axial position, from 7–10 measurement zones were sampled circumferentially between suction and pressure surfaces. Each of these zones include all velocity measurements in a gated encoder window of 1/20 of the arc length between adjacent blade suction surfaces. The above series of measurements were repeated at 50.0, 62.5, 75.0, and 90.0% span.

Geometric considerations prevented taking data at much less than 50% span; therefore measurements were not ob-

tained near the hub, and signal-to-noise ratio (SNR) considerations limited how close measurements could be made to the tip. Reduced SNR was especially noticeable in the violet signal. Internal reflections from the window and the scattering of light from seed accumulating on the window combined to create flare in this region. Frequent washing of the window helped to reduce the noise, but 7 mm (91% span) was the closest to the window that a measurable signal could be extracted from the violet channel. Measurable signals could be obtained in the blue and green channels as close as 5 mm (94% span) from the window.

The data rate on the violet channel was in general from 5 to 8 times lower than either the blue or the green, and the violet channel was always the most sensitive to filtering. While the maximum data rate on the blue and green channels was about 500 per s, the violet channel rarely recorded above 100 per s. Signals from the blue channel were usually of higher quality than those from the green.

With careful attention to filtering and frequency shift, the quality of the data, as reflected in the velocity histograms, was equal in all three channels at most locations. Representative histograms are shown in Fig. 3. The standard deviation of the measured components is from 1.7 to 2.0 m/s at most locations, independent of either the total velocity or component velocity. In general, an entire span of data (49–70 positions throughout the blade passage with 1024 measurements on each of the three channels) could be obtained in from 6–8 h.

The velocity measurements, though made in the stationary frame of the laboratory, are presented in the rotating frame of the rotor—that is, the blade velocity was subtracted from the total measured velocity for clarity of presentation. The velocity measurements in the relative frame of the blades are presented in two types of vector plots. The first is simply a projection of the relative velocity vector on the  $x$ - $t$  plane. Thus, these plots show the axial and relative tangential velocities.

The second type of plot shows the relative flow in the  $t$ - $r$  plane as described in Moore and Moore.<sup>12</sup> The secondary flow is defined as follows. First, a primary flow,  $V_1$  is defined. The primary flow direction is constrained to lie in the  $x$ - $t$  plane and is set at an angle  $\alpha$  to the horizontal given by

$$\alpha = \alpha_s + \frac{h_{ms}}{h_{ps}} (\alpha_p - \alpha_s) \quad (2)$$

where the horizontal plane contains the axis of the rotor and

the normal to the optical window. All variables have been defined at the measurement span and chord locations. Thus, the direction of the primary flow varies linearly with distance between the pressure and suction surfaces.

The secondary flow,  $V_2$  is constrained to lie in the  $t$ - $r$  plane. With the primary and secondary flows thus constrained, there exists one and only one pair of vectors,  $V_1$  and  $V_2$  which sum to a given relative velocity. This is illustrated in Fig. 4.

The projection of the relative velocity vectors at 50% span on the  $x$ - $t$  plane is shown in Fig. 5. From this figure it is observed that measurements were obtained over almost the entire blade passage. There were only two regions in which data could not be obtained. First, there was a small volume below the pressure surface which was shadowed from view by the blades. Second, no measurements could be made in the blade wake. The data rate in the wake dropped to zero.

It is believed that the loss of data in the near-wake of the rotor blades was due to seed depletion caused by turbulent mixing in the wake with consequent entrainment of unseeded adjacent fluid. It was suggested by a reviewer that an alternative explanation is the inability of the seed particles to flow the sharp gradients in the near-wake region coupled with the tendency of the particles to centrifuge away from the suction surface. This suggestion is not disputed. The hypothesis that entrainment of unseeded fluid was responsible for loss of data in the near-wake is based upon 1) the experience here that the data rate at any location was found to be very sensitive to the upstream local seed injection position. That is, the upstream seeding is perhaps excessively local. Minor adjustments in this position resulted in large changes in data rate. 2) Turbulence measurements (not reported here) indicate a large increase in turbulent energy near the suction surface beyond 50% axial chord and in the region downstream of the blade row. Because of seed production rate limitations and the inability to contain the compressor exhaust satisfactorily, full inlet seeding, which would test the depletion hypothesis, was not attempted during these series of tests. As the wake region is of great interest, this question should be resolved in future experiments.

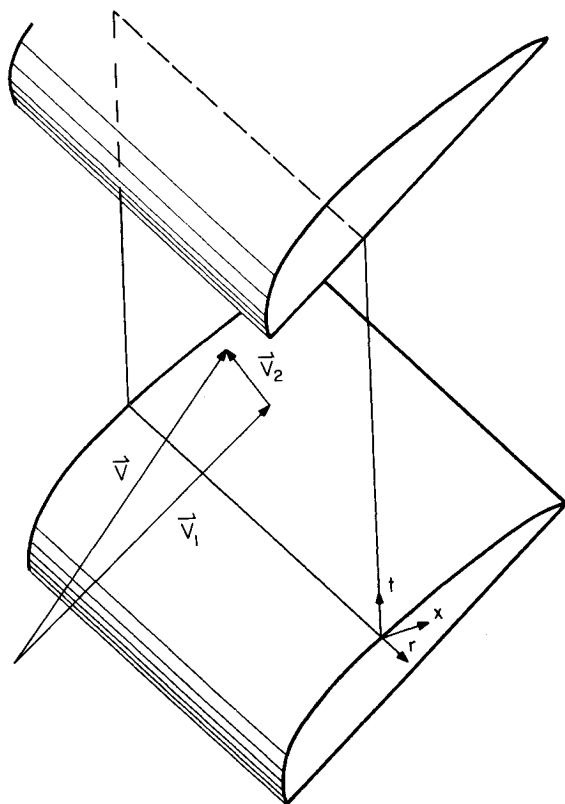


Fig. 4 Secondary flow definition.

Figure 5 shows the flow at 50% span to be well behaved. The flow accelerates over the suction surface following the contour of the blade. Although the encoder window extended to the suction side surface, little or no velocity deficit is shown in the measurements just above the suction surface. The encoder window is sufficiently large compared to the boundary-layer thickness, and the number of measurements inside the boundary layer is small compared to the number of measurements in the free stream.

For comparison purposes, a two-dimensional potential flow solution was computed for this blade profile at 50% span using the measured upstream velocity (which is well approximated as uniform). The measured axial/relative tangential velocities are in nearly complete agreement with the potential flow model. Small differences (primarily in relative flow vector angle) are present beyond 50% axial chord, particularly near the suction surface. The potential flow results along the suction surface were also used to compute the boundary-layer development. The computed boundary-layer growth is small compared to the gated encoder window and is insufficient to account for the differences between the computed potential flow behavior and the measured velocities. It is noted however that the rotor/stator interaction was not included in the potential flow model and, as will be shown shortly, a significant flow disturbance near the blade tip is present, which may be affecting the flowfield away from the tip.

Figure 6 shows the projection of the velocities at 90% span in the  $x$ - $t$  plane. Planes between 50 and 90% span are similar in character to the 50% results and are not included due to space limitations. The flow at 90% span is not as well behaved as at the lower span locations. Measurements in the blade passage were difficult to obtain at this span, especially near the blade suction surface where the turbulence was very high. At 22% and 42% axial chord, the combination of high turbulence and low SNR made it impossible to obtain data near the suction surface. Over most of the blade passage, the variance of the measured components was only 10–25% greater than at spans further from the tip. However, near the blade suction surface, the standard deviation of the velocity components was from 3–5 m/s on all channels. This is serious for the green

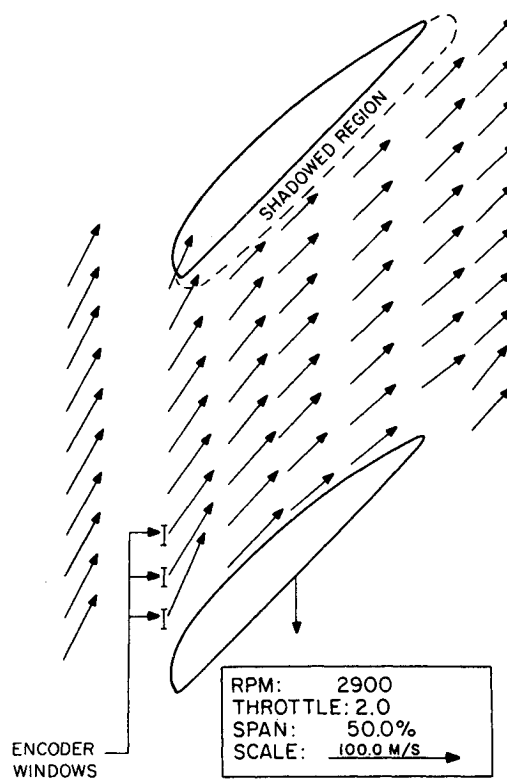


Fig. 5 Relative velocity,  $x$ - $t$  view, 50% span.

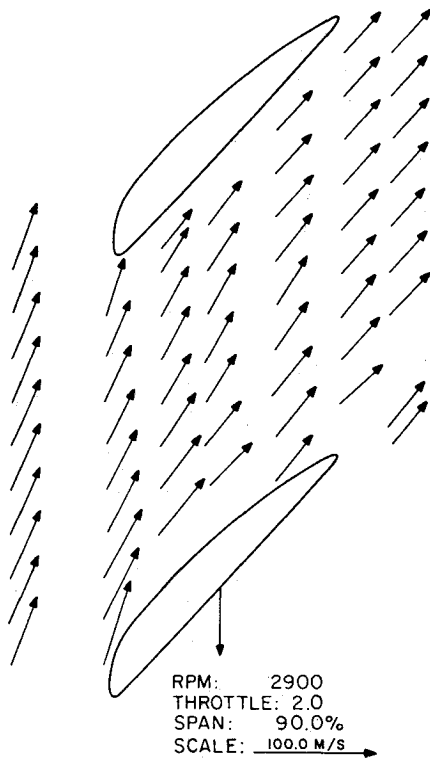


Fig. 6 Relative velocity,  $x-t$  view, 90% span.

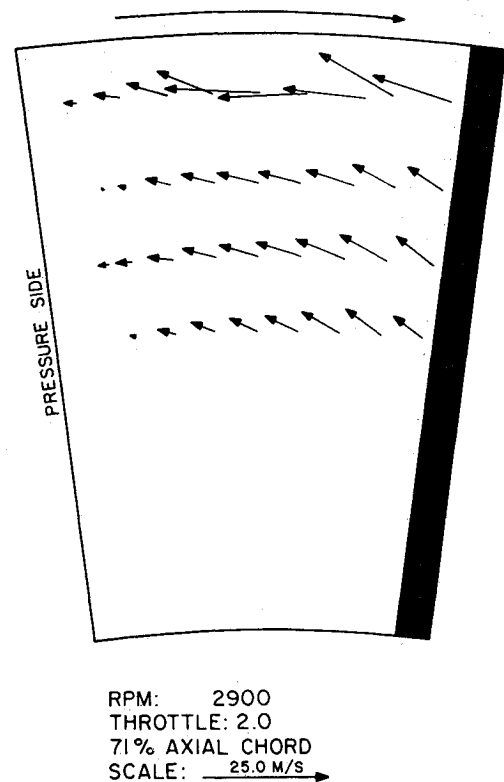


Fig. 8 Relative secondary flow, 71% axial chord.

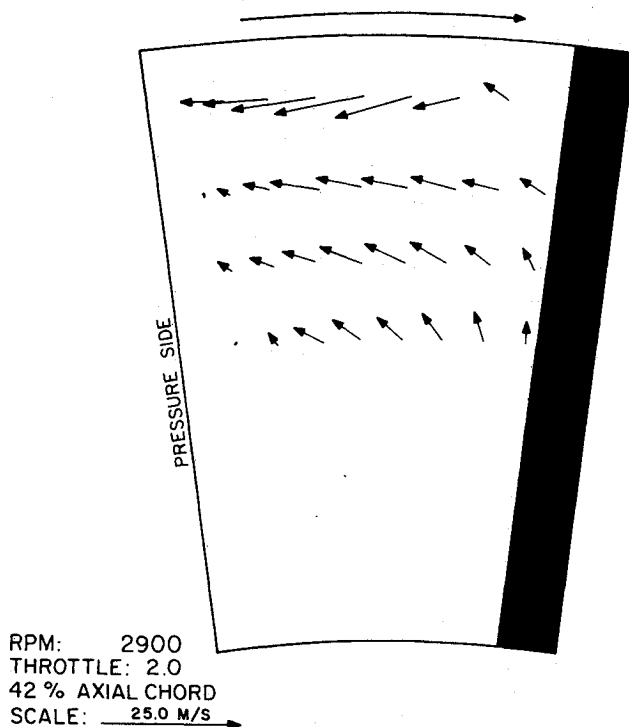


Fig. 7 Relative secondary flow, 42% axial chord.

and violet channels near the suction surface as the mean velocities are on the order of 5–10 m/s at this location. The authors agree with a reviewer that a likely explanation for the results at 90% span is the presence of flow separation on the suction surface, perhaps with reattachment (a separation bubble). This would be consistent with the poor SNR and low data rate since all but the “very small particles are centrifuged out of the bubble.”

The secondary velocities are shown in Figs. 7 and 8. These show that, in general, the flow is moving radially outward and

that there is a gradient of the radial flow from suction to pressure side. The radial velocity is near zero for all plots near the pressure side. It is interesting to note that at 42% axial chord, the flow follows closely to the blade suction surface, but at 71% axial chord, there is a significant component of the velocity moving away from the blade surface. This departure from the suction surface extends across the entire measured span. This is not accounted for by the boundary layer growth (based upon the calculation using the potential flow solution). Again, this behavior where the flow appears unable to follow the blade turning may be the result of stator-rotor interaction or it may be influenced by the flow disturbance in the tip region discussed previously. Without further study, this behavior is not unequivocally explained.

From the previous figures and uncertainty results, it is clear that the LDA system is capable of making detailed measurements of the three dimensional motion inside the moving blade passages. Importantly, the weak secondary motion is resolved and indicates a dominant outward radial flow with some indication of circulation; although unfortunately back flow toward the hub was not measured due to shadowing near the pressure surface where back flow is occurring. In order to verify and substantiate the motions which were measured, a simple analysis was made of the secondary motion.

The gradient of the radial velocity across the blade passage was examined by simple irrotational considerations. From Dring, Joslyn, and Hardin,<sup>13</sup> flow that is irrotational in the absolute frame will have a relative vorticity of  $2 \times \Omega$  in the rotating frame outside of the regions influenced by viscosity. The  $\Omega$  is the angular velocity of the rotor. This relative vorticity results in the following phenomena: a gradient of radial velocity across the blade passage or a gradient of the product  $rV_\theta$  across the blade span. Only if the flow is a free vortex will there be no gradient of radial velocity.

That is, for irrotational flow (in the absolute frame):

$$\nabla \times \mathbf{V} = 0$$

(3)

and it follows that

$$\frac{1}{r} \frac{\partial}{\partial r} (rV_\theta) - \frac{1}{r} \frac{\partial V_r}{\partial \theta} = 0 \quad (4)$$

For free vortex flow

$$\frac{\partial}{\partial r} (rV_\theta) = 0 \quad (5)$$

and in this event there is no gradient in the radial velocity.

The blades in this machine do not produce a free vortex flow; therefore a gradient in the radial velocity is expected. When the measured velocities are numerically differentiated so as to compute the gradients of tangential and radial velocities, it is found that in fact the measured gradient in radial velocity is exactly that needed to maintain irrotationality in the stationary frame. Thus the gradient of the radial velocity across the flow is explained.

The mean outward radial flow is not accounted for by this theory, however. To explain the average radial component of the measurements, the pressure probe measurements discussed previously were reconsidered. As was noted, the three-hole probe measurements indicated a movement of flow radially outward through the blade passage based on continuity considerations. From the pressure probe measurements, an average radial velocity through the blade passage can be estimated. This estimated average radial velocity is in good agreement with the radial velocity measured with the LDA.

Thus the radial-flow structure inside the blade passage is the result of two effects. First, due to the deviation of the flow from that of a free vortex, a gradient of radial velocity from suction to pressure surface is induced. Second, a global radial flow outward is present, as dictated by continuity, when the essentially uniform mass flux at the entrance to the blade passage is skewed toward higher mass flux in the blade tip region at the passage exit.

### Conclusions and Recommendations

The objective of this research was to examine the suitability of a three-color, three-component laser Doppler anemometer for measuring simultaneously all components of the instantaneous velocity inside turbomachinery blade passages. Based upon the presented results, it is concluded that simultaneous three-component velocity measurements via LDA in the confined blade passages of operating axial-flow compressors is practical. Comparisons of such measurements in a low-speed compressor with three-hole pressure probe measurements, two-dimensional potential flow calculations, and an irrotational flow approximation in the core of the blade passage indicate that both the dominant axial/tangential flow measurements and the secondary flow in the tangential/radial plane are consistent with these other measurements and calculations. In the present case, the relative uncertainties in the mean axial and tangential velocities were a few percent, whereas the mean radial velocity relative uncertainty was on the order of 10–20%. The relative uncertainty was less than 2% of the total velocity.

Therefore, it is concluded that accurate simultaneous three-component measurements are possible and practical for the study of the three-dimensional velocity field inside these machines.

The results of this work and the experience gained from this application also revealed some problems with measurements at specific locations within the blade passage and with measurements if blade passage-to-blade passage studies are desired. The paper concludes with a brief discussion of the problems which must be addressed in the future and with recommendations for measurement system improvement.

For the most part, there were no difficulties in making the LDA measurements within the blade passage. Measurements

near the blade suction surface were not significantly more noisy (off-axis scatter may have helped in this regard) nor was the data rate seriously reduced near the blade suction surface. Difficulty was experienced 1) in the blade wake, 2) near to the optical window (at less than 7 mm from the inside surface), and 3) with the data rate in general throughout the blade passage particularly in the 476.5 nm channel.

The primary limitation of this system was the low data rate of the violet channel. Since, for detailed total-velocity vector measurements using nonorthogonal measured components, it is highly advantageous to use the coincidence mode of data collection, the low violet data rate limits the entire system. For the data collection scheme used for these measurements, the data rate on the violet channel was on the order of 60 per s. At these same conditions, the data rate on the blue and green channels was typically 200–300 per s. If a single passage were to be examined using the same size encoder window, the data rate would drop to about 2 per s on the violet. Smaller encoder windows would result in yet a lower data rate. With these low data rates, the time to collect data is prohibitive. As the ultimate use of these measurement systems is to make detailed measurements inside individual blade passages and in the blade wakes, etc., this limited data rate must be improved if practical and technologically interesting flows are to be studied.

The data rate problems in the violet channel apparently were caused by poor SNR, which is believed to be the result of low power in the violet beams. There are several ways in which this problem can be reduced. First, a greater amount of seed must be introduced to the flow. This is needed in any case to obtain a higher data rate in the other channels and in the blade wake region. The use of higher output seeders or seeding the entire flowfield, however, would not improve the SNR in the violet channel. Thus, high-noise regions, such as near the window and hub, would still present problems.

Second, monodisperse seed should be used with the seed size determined such that SNR is large for the LDA collection optics that are employed. The seed size and LDA optical arrangement must be determined by a compromise between optical access, SNR, measurement uncertainty, and particle lag. In the present work, polydisperse sugar seed was used primarily for health considerations, and no attempt was made to enhance the data rate by improving SNR with adjustments in seed size or LDA geometry.

It is also recommended that the violet fringes be oriented so that they are at the most advantageous position to measure a particle. As the flow in this compressor moves through the blade passage, it becomes very close to being parallel to the violet fringes. Due to angular bias considerations, this causes a low probability of making a measurement on a particle in the violet channel. Increasing the frequency shift reduces accuracy and SNR. The probability of making a measurement on a particle with the blue channel, though, is always high, since as the flow attains swirl, the particle path approaches a normal to the fringes. If the positions of the three beams were rearranged—with the violet measuring the component that the blue measured and either the green or the blue set to measure the component measured by the violet—the violet signal would improve, and the data rate would increase. The signal of the color replacing the violet would, of course, suffer, but the power in both the blue and green beams is high, and the effect would not be as serious as for the violet. In this way, the weakest color would be placed in the most advantageous position, and the strongest color would be placed where the most power is needed.

Another promising technique for improving the violet data rate is to use a new frequency domain signal processor such as described by Arik and Buchhave.<sup>14</sup> The advantage of this processor is that an fast Fourier transform (FFT) analysis of the frequency is much less sensitive to noise than a counter type frequency measurement. Arik and Buchhave report making measurements down to an SNR of –6 dB, a full 15 dB

lower than counter-type processors. Instruments based upon this principle should significantly improve the data acquisition in the violet channel.

Finally, the last method of improving the signal in the third component is to increase the power of the beams. A second argon ion laser for the violet wavelength could be introduced. Two separate lasers, one tuned to the green and blue colors and one tuned solely to the violet, would provide more power in all channels. This solution for low beam power has appeared in the literature.<sup>15</sup>

A combination of switching the position of the three colors to minimize the disadvantage of low violet power and the use of frequency domain burst processors to decrease the sensitivity to signal-to-noise problems is an attractive solution to the limitations of this system. If these two changes are implemented and sufficient seed is introduced, it should be possible to make three-dimensional flow measurements both with high accuracy and high data rate in many turbomachinery applications.

### Acknowledgment

This work was sponsored by the United States Air Force, Wright-Patterson Air Force Base. Contract F 33615-85-C-2575/SB5851-0358 and subcontract with Universal Energy Systems, Dayton, Ohio.

### References

- <sup>1</sup>Strazisar, A. J., "Application of Laser Anemometry to Turbomachinery Flowfield Measurements," von Kármán Lecture Series No. 3, 1985.
- <sup>2</sup>Stauter, R. C., and Fleeter, S., "LDA Measurement of the Passage Flow Field in a 3-D Airfoil Cascade," AIAA Paper 86-0501, 1986.
- <sup>3</sup>Carey, C., Fraser, S. M., and Wilson, G., "Behavior of Air in a Mixed-Flow Rotor Operating at Off-Design Duty Points," *ASME International Symposium on Laser Anemometry*, American Society of Mechanical Engineers, New York, 1985, pp. 27-33.
- <sup>4</sup>Dancey, C. L., "A Review of Three-Component Laser Doppler Anemometry," *International Journal of Optical Sensors*, Vol. 2, No. 6, 1987, pp. 437-469.
- <sup>5</sup>Meyers, J. F., "The Elusive Third Component," *ASME International Symposium on Laser Anemometry*, 1985, pp. 247-254.
- <sup>6</sup>Ng, W. F., O'Brien, W. F., and Olsen, T. L., "Experimental Investigation of Unsteady Fan Flow Interaction with Downstream Struts," *Journal of Propulsion and Power*, Vol. 3, No. 2, 1987, pp. 157-163.
- <sup>7</sup>Kreid, D. K., "Laser-Doppler Velocimeter Measurements in Nonuniform Flow: Error Estimates," *Applied Optics*, Vol. 13, No. 7, Aug. 1974, pp. 1872-1881.
- <sup>8</sup>Durst, F., Melling, A., and Whitelaw, J. H., *Principles and Practice of Laser Doppler Anemometry*, 2nd ed., Academic, London, 1981.
- <sup>9</sup>Chesnakas, C., "Total Velocity Vector Measurements in an Axial-Flow Compressor Using a 3-Component Laser Doppler Anemometer," Masters Thesis, Dept. of Mechanical Engineering, Virginia Polytechnic Institute and State University, Blacksburg, VA, 1988.
- <sup>10</sup>Neti, S., and Clark, W., "On-Axis Velocity Component Measurement with Laser Velocities," *AIAA Journal*, Vol. 17, No. 9, 1979, p. 1013.
- <sup>11</sup>Petrie, H. L., Samimy, M., and Addy, A. L., "An Evaluation of LDV Velocity and Fringe Bias Effects in Separated High Speed Turbulent Flows," *International Congress on Instrumentation in Aerospace Simulation Facilities Record*, 1985, pp. 297-308.
- <sup>12</sup>Moore, J., and Moore, J. G., "Secondary Flow, Separation and Losses in the NACA 48-Inch Centrifugal Impeller at Design and Off-Design Conditions," ASME Gas Turbine Conference, American Society of Mechanical Engineers, New York, June, 1988.
- <sup>13</sup>Dring, R. P., Joslyn, H. D., and Hardin, L. W., "An Investigation of Axial Compressor Rotor Aerodynamics," *Transactions of the American Society of Mechanical Engineers, Journal of Engineering for Power*, Vol. 104, Jan. 1982, pp. 84-96.
- <sup>14</sup>Arik, E. B., and Buchhave, P., "Burst Spectrum Analyser: A Unique Signal Processor with Unique Applications," *Sixth International Congress on Application of Lasers and Electro-Optics*, San Diego, November, 1987.
- <sup>15</sup>Pfeifer, H. J., "A New Optical System for Three-Dimensional Laser-Doppler-Anemometry Using an Argon-ion and a Dye Laser," *International Congress on Instrumentation in Aerospace Simulation Facilities Record*, 1985, pp. 56.